NUMERICAL SIMULATION FOR HEAT TRANSFER OF SILICA-AEROGEL FILLED 3-D STITCHED SPACER FABRIC COMPOSITES

by

Tianjiao LIU [a], ***Ning LI*** [a,c], ***Mengqi TIAN*** [a,d], ***Jie DONG*** [b], ***Mu YAO*** [b], ***Runjun SUN*** [b*], ***and Yujuan Li*** [b]

[a] College of Textile and Clothing Engineering, Soochow University, Suzhou, China
[b] School of Textile Science and Engineering, Xi'an Polytechnic University, Xi'an, China
[c] College of Apparel and Art Design, Xi'an Polytechnic University, Xi'an, China
[d] School of Science, Xi'an Polytechnic University, Xi'an, China

Original scientific paper
https://doi.org/10.2298/TSCI220917027L

Spacer fabrics and their composites have great advantages of being excellent heat insulation materials because of their cavity structure characteristics. However, there are few researches on the thermal insulation of spacer fabric composites with different spacer shapes and geometric parameters. In this work, stitched spacer fabric composites filled with silica aerogel with rectangular, triangular and trapezoidal spacer shapes and their models were designed. The results of experiments and simulations show that the temperature distribution of spacer fabric composites has good consistency at high temperature. By analyzing the heat transfer results of composites with different geometric parameters, it was found that the length of the connecting layer between the top and bottom layers and the distance between two adjacent sutures in the top layer affect the minimum and maximum temperatures of the top surface.

Key words: *numerical simulation, spacer fabric, silica aerogel, heat transfer, basalt fiber fabric, thermal insulation*

Introduction

Spacer fabric is a 3-D fabric whose surface layer is connected with the surface layer by yarn or fabric, forming a space in the vertical direction of the fabric according to a certain rule [1, 2]. According to the production process, spacer fabric can be divided into three categories: woven spacer fabric, knitted spacer fabric, and stitched spacer fabric [3-5]. Spacer fabric and its composite materials have the characteristics of high strength, high elastic modulus, good pressure resistance, impact resistance, heat insulation and light weight, and have a wide range of applications in construction, thermal protection, automobile, medicine and aerospace [6-10].

By using the fabric as a spacer of intermediate connecting layers, the cross-sections of the spacers can be designed into various shapes, such as trapezoids, triangles and rectangles, as needed. The composite material made of this spacer fabric has excellent mechanical properties. Neje and Behera [11] designed spacer fabric composites with three different spacer shapes: rectangle, trapezoid and triangle, and studied the transverse compression properties of

* Corresponding author, e-mail: sunrunjun@xpu.edu.cn

spacer fabric composites with different spacer shapes. In the following research, Neje and Behera [12] found that the change of the geometric parameters of the spacer shape will affect the mechanical properties of the spacer fabric composites to a certain extent. The researchers also made composites by filling the cavities of the spacer fabric with thermal-insulating material. Wang *et al.* [13] designed several spacer fabrics with different structures using glass fiber and found that the spacer fabric composite filled with silica had good thermal insulation ability. Many researchers have studied on the mechanical properties of spacer fabric composites with different spacer shapes and different geometric parameters. However, there are few papers on the influence of those on the thermal insulation of spacer fabric composites.

In this work, to study the influence of different spacer shapes and different geometric parameters on the thermal insulation of spacer fabric composites is the main purpose. The basalt fiber yarns were used to weave plain fabrics. In order to control the geometric parameters accurately, three kinds of spacer fabrics with different spacer shapes of rectangle, triangle and trapezoid were prepared by suture. Silica aerogels were filled in the gap of spacer fabric to prepare the composites with thermal-insulation ability. In the COMSOL5.5, the corresponding models were established according to the geometric parameters of the spacer fabric composites. The heat transfer processes of the models at 773.15 K were also analyzed. The experimental equipment was designed and the results of numerical simulation were verified by experiments. Finally, the effects of different spacer shapes and geometric parameters on the thermal insulation of spacer fabric composites were analyzed by simulation and experiment. This provides some reference value for the design, optimization and application of spacer fabric composites in the field of thermal insulation.

Methodology

Preparation of 3-D stitched spacer composites and geometrical models

Basalt fiber yarn was purchased from Sichuan Juyuan Basalt Fiber Technology Co., Ltd., China. Fiber's diameter of the basalt yarn was 17 μm. The plain-woven fabric was woven by the basalt yarn on a small sample loom (SGA598, Tongyuan, China). The thickness was measured by a fabric thickness gauge (YG141D, Jigao, China). The specifications of the woven fabric are listed in tab. 1.

Table 1. Basalt woven fabric specifications

Fabric structure	Warp sett [per 10 cm]	Weft sett [per 10 cm]	Thickness [mm]	Yarn linear density [tex]	Areal density [gm^{-2}]
Plain	80	78	0.35	240	390.90 ±7

The 3-D stitched spacer fabrics were sutured by two separate plain-woven fabric layers which were up and down and a plain-woven fabric layer connected in the middle. All the plain-woven fabric layers were woven by the basalt yarn. A kind of basalt fiber yarn which was purchased from Sichuan Juyuan Basalt Fiber Technology Co., Ltd., China was used to be the suture. The yarn's linear density and the fiber's diameter of the yarn were 85 tex and 9 μm. The spacer's shapes of the 3-D stitched spacer fabrics were designed as rectangle, triangle and trapezoid. The shorthand notations of samples with different spacer shapes were marked as REC, TRI, and TPZ, respectively in the following. The cross-section's schematic diagrams of the 3-D stitched spacer fabrics are shown in fig. 1.

In fig. 1, the top length side of rectangle and the topline of trapezoid were defined as a, the bottom length side of rectangle, the base of triangle and the baseline of trapezoid were defined as b, the base angle between the bottom layer and the connecting layer was defined as θ.

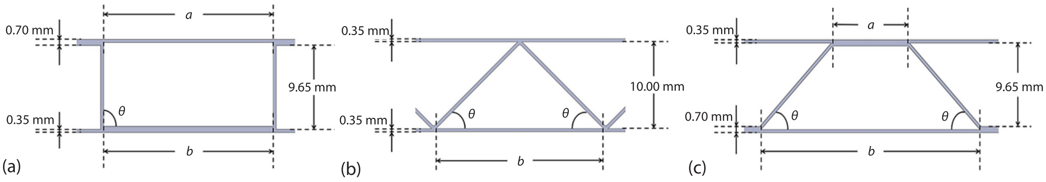

Figure 1. The cross-section's schematic diagrams of the 3-D stitched spacer fabrics; (a) rectangle, (b) triangle, and (c) trapezoid

In this work, a series of geometrical parameters of the 3-D stitched spacer fabrics with the three different spacer's shapes were designed. The geometrical parameters are shown in tab. 2.

Table 2. The geometrical parameters of the 3-D stitched spacer fabrics

Sample	a [mm]	b [mm]	θ
REC5	5.00	5.00	90°
REC10	10.00	10.00	90°
REC15	15.00	15.00	90°
REC20	20.00	20.00	90°
REC25	25.00	25.00	90°
TRI15°	0	72.00	15°
TRI30°	0	33.43	30°
TRI45°	0	19.30	45°
TRI60°	0	11.14	60°
TRI75°	0	5.17	75°
TPZ5	5.00	24.30	45°
TPZ10	10.00	29.30	45°
TPZ15	15.00	34.30	45°
TPZ20	20.00	39.30	45°
TPZ30°	10.00	43.43	30°
TPZ45°	10.00	29.30	45°
TPZ60°	10.00	21.14	60°
TPZ75°	10.00	15.17	75°

The 3-D stitched spacer fabric is a combination of fiber and air. In order to simplify the model and improve the computing efficiency, the fabric assembly was modeled as a whole by using COMSOL 5.5, and on the basis of the actual fabric geometric parameters and spacer's shapes. Some sketch maps of the 3-D stitched spacer fabrics and their corresponding models are shown in fig. 2.

The spacers of the 3-D stitched spacer fabrics were filled with pure silica aerogel purchased from Langfang Yvao Energy Saving Technology Co., LTD., China. The final model diagram of 3-D stitched spacer composite filled with silica aerogel is shown in fig. 3.

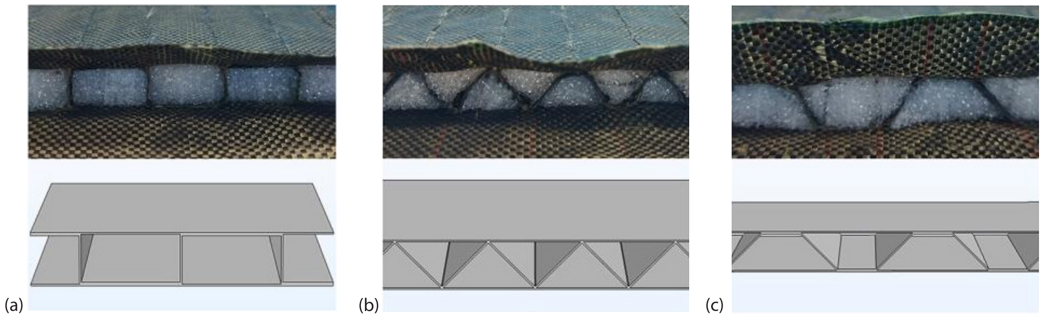

Figure 2. Sketch maps of the 3-D stitched spacer fabrics and their corresponding models; (a) REC20, (b) TRI45°, and (c) TPZ10 (TPZ45°)

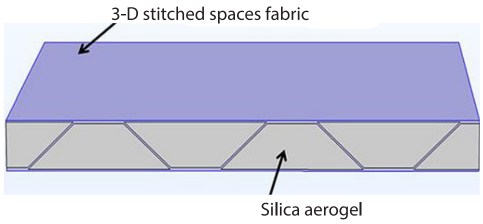

Figure 3. The final model diagram of 3-D stitched spacer composite

Numerical simulation method

Heat transfer equation

In COMSOL5.5, the equation of steady-state heat transfer can be described:

$$\rho C_p \vec{\mu} \nabla T + \nabla\left(-k \nabla T\right) = Q \tag{1}$$

where ρ, C_p, and k are the density, specific heat capacity, and thermal conductivity of material, respectively, T – the temperature, Q – the heat source, and $\vec{\mu}$ – the velocity vector. According to the eq. (1), the densities, specific heat capacities and thermal conductivities of 3-D stitched spacer composite models need to be set.

Material thermophysical parameters

The 3-D stitched spacer composite model contains fabric and silica aerogel two parts. In this work, the models of fabric and silica aerogel are considered isotropic materials in order to simplify numerical simulation. For any material, there is a dependent relationship between thermal conductivity and temperature. Therefore, in order to accurately simulate the steady-state heat transfer of 3-D stitched spacer composite at high temperature, this property of material cannot be ignored. In the numerical simulation, the specific heat capacity and density of the

Table 2. The thermophysical parameters of silica aerogel

Temperature [K]	Thermal conductivity [14] [$Wm^{-1}K^{-1}$]	Specific heat capacity [15] [$Jg^{-1}K^{-1}$]	Density [kgm^{-3}]
293.15	0.0235	0.85	53
573.15	0.0400		
773.15	0.0575		

material were assumed to be constant independent of temperature. The thermophysical parameters of silica aerogel and fabric are shown in tabs. 2 and 3, respectively. Since silica aerogel is in powder form, the measured density is tap density.

Table 3. The thermophysical parameters of fabric

Temperature [K]	Thermal conductivity [16] [$Wm^{-1}K^{-1}$]	Specific heat capacity [16] [$Jg^{-1}K^{-1}$]	Density [kgm^{-3}]
293.15	0.430	0.697	1434.3
457.15	0.608		
617.15	0.781		
777.15	0.905		

Boundary conditions

The direction of heat transfer in the 3-D stitched spacer composite was set to along the fabric thickness. The initial temperature of the model was set to 293.15 K which was the room temperature at that time. The boundaries of models were considered as thermal insulated. A heating temperature load of 773.15 K was set to the bottom surface of the models.

It was well known that the main ways of heat transfer are heat conduction, heat radiation and heat convection. According to eq. (1), heat conduction is the main heat transfer form in this simulation work. Since the thermal conductivity parameter used in this work takes into account the influence of temperature, and the influence of high temperature on thermal conductivity includes thermal radiation, it was reasonable to not consider thermal radiation again in this work. Therefore, thermal convection between the air and the boundaries of 3-D stitched spacer composite also needs to be taken into account. In COMSOL5.5, the convective heat flux, q_0, is defined:

$$q_0 = h\left(T_{\text{ext}} - T\right) \tag{2}$$

where h is the convective heat transfer coefficient, T_{ext} – the external temperature, and T – the temperature of the top surface of the 3-D stitched spacer composite. The convection heat transfer coefficient of the top surface on the 3-D stitched spacer composite was set to 15 W/m^2K [17].

Meshing

In order to grid the stereo model accurately, regular tetrahedron was selected as the unit of grid. The selection of mesh size affects the accuracy and operation time of numerical simulation. After multiple comparisons, the *refinement* option under the physical field control grid in the software was selected to grid the models. The cell size of the grid in the models ranges from 0.8-8 mm. Through the refinement research, it was found that the minimum cell quality of the mesh is greater than 0.1, which shown that the overall grid quality is feasible.

Experimental verification

The experimental device's diagram for verifying the experiment is shown in fig. 4. The heating device was supplied by Xuankang Electric Heating Appliance Co., Ltd., China. First, the temperature of the heating plate was set to 773.15K by the heating device. Then, the 3-D stitched spacer composite was placed in the center of the heating plate when the temperature of the heating plate was steady. The infrared thermometer (869, Testo, Germany) was placed 20 cm approximately above the 3-D stitched spacer composite to observe the tempera-

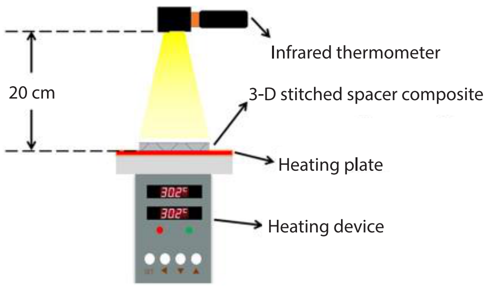

Figure 4. The experimental device's diagram

ture distribution on the top surface of the composite. When the temperature distribution of the composite reached a stable state, the temperature distribution of the upper surface of the 3-D stitched spacer composite was shot with infrared thermometer.

Results and discussion

The results of experimental verification

The top surface's temperature distributions of the 3-D stitched spacer composites and the corresponding models under the heating temperature is shown in the fig. 5. In order to better compare the thermal insulation's effect of composites with different spacer's shapes, and compare the simulation results and experimental results, a series of nodes along the *x*-axis were selected on the top surface of the composites. The method of selecting nodes which were located on the different positions of the top surface and in regular order is shown in fig. 6. Temperature curves were drawn according to the temperatures of the selected nodes.

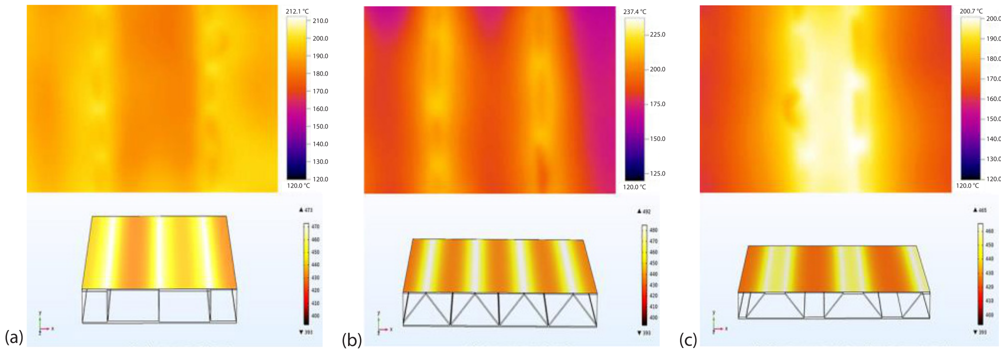

Figure 5. The temperature distributions of experimental results and simulation results; (a) REC20, (b) TRI45°, and (c) TPZ10 (TPZ45°)

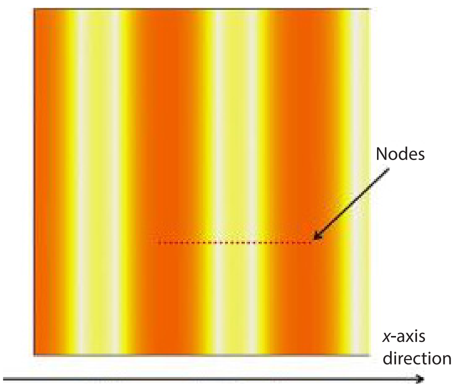

Figure 6. Schematic diagram of selected nodes

The top surface's temperature curves are shown in fig. 7. The simulation results were very close to the experimental results from the temperature values and curve rules, and it was also found that the maximum relative error between the simulated value and the experimental value is about 4.8%, which also showed that the heat transfer simulation of the 3-D stitched spacer composites in this work was feasible. The maximum temperature of the top surface of the 3-D stitched spacer composites was generally located on the suture of the connecting layer and the top layer. This is because the thermal conductivity of the fabric is much greater than that of aerogel, so the heat from the bottom layer is more easily transferred to the top layer along the connecting layer in the middle. This also shows that the filled silica aerogels have a good effect on thermal insulating. By comparing the maximum temperatures of the top surfaces of the three kinds of 3-D stitched spacer composites with different spacer's shapes, it can be found that the temperature reached at the top surface of the composite with triangle shape is the highest. This is because that the heat from two paths from the bottom layer to the top layer of the composite gathers at the same suture on the top surface, resulting in the maximum temperature of the composite with triangle shape bigger than that of other composites.

The fig. 7 shows that the minimum temperature of the top surface of the 3-D stitched spacer composites with the rectangle and triangle shapes is located in the middle of the two adjacent sutures. But the minimum temperature of the top surface of the 3-D stitched spacer composite with the trapezoid shape occurred on the middle of the trapezoid's baseline. It can be seen from the data in fig. 7 that the minimum temperature of the top surface of the composite with trapezoid shape is the lowest.

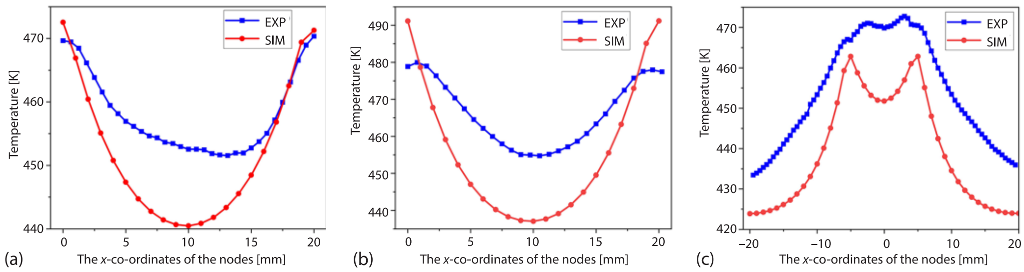

Figure 7. (a) The temperature curves of REC20, (b) TRI45°, and (c) TPZ10 (TPZ45°)

To explore different geometry parameters in the influence of 3-D stitched spacer composites on the thermal insulation, numerical simulation method was used in this work to study the impact of the value changes of the top length side of the rectangle, the base angle of the triangle, the topline and the base angle of the trapezoid on thermal insulation effect of 3-D stitched spacer composites with corresponding spacer shape.

The length of the rectangle's length side

The simulation temperature curves of the selected nodes on the top surface of the composites with different lengths of the rectangle's top length sides are shown in fig. 8(a).

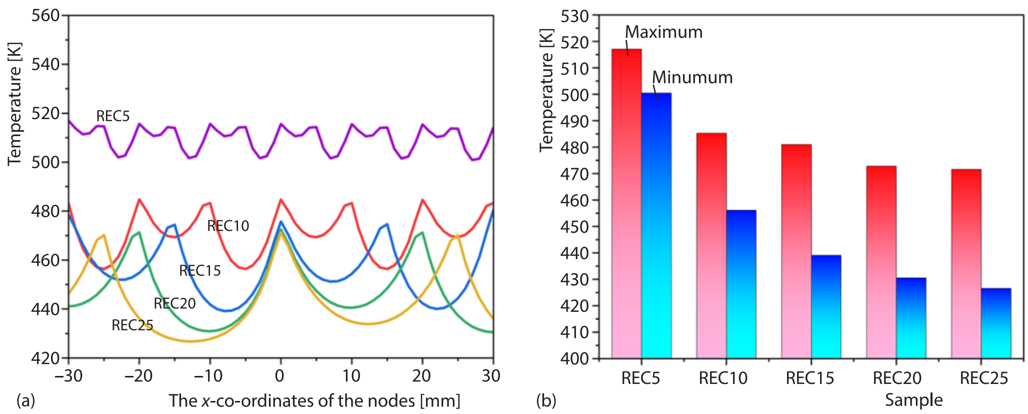

Figure 8. (a) Simulation temperature curves of composites with different the rectangle shape's top length sides and (b) maximum and minimum temperature of the top surface of the rectangle-shape's composites with different lengths of top length sides

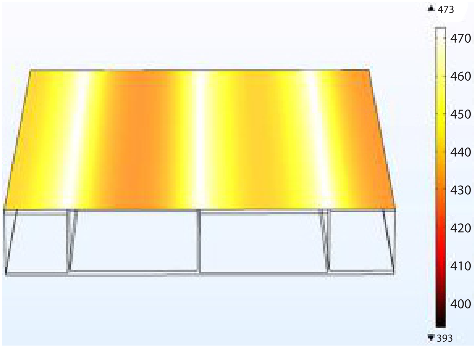

Figure 9. The simulation result of the composite with the rectangle shape

The maximum temperature of the top surface of the composites occurred on the suture between the connecting layer and the top layer, and the values of maximum temperature on each place of the top surface were nearly consistent. The minimum temperature of the top surface of the composites was located in the middle of the rectangle's top length side. But it can be seen from fig. 9, the values of the two adjacent minimum temperatures were not the same, and when the connecting layer was combined with the top layer the minimum temperature was higher than that of the single top layer. This might be due to the fact that when heat transferred from the connecting layer to the top surface suture, it continued to transferring through the fabric on either side of the top surface suture. The top surface of a double-fabric layer tended to transfer more heat than that of a single-fabric layer.

It can be seen from fig. 8(b), as the length of the top length side increases, the minimum temperature of the top surface of the rectangle-shape's composite decreases. This was due to the increased length of the top length side, which increased the heat transfer path from the suture on the top surface to the either side, thereby reduced the amount of heat reaching the middle of the top length side. It can also be found that when the length of the top length side was 5 mm, the maximum temperature of the top surface of the rectangle-shape's composite was far greater than that of other composites. This was because when the length of the top length side was small enough, the heat from the sutures to the either side easily and then reached the adjacent suture, caused the other maximum temperature's value to rise.

The degree of the triangle's base angle

The simulation temperature curves of the selected nodes on the top surface of the triangle-shape's composites with different degrees of the triangle's base angles are shown in fig. 10(a). The maximum temperature of the top surface of the composite was located on the suture and the minimum temperature was located in the middle of the triangle's baseline.

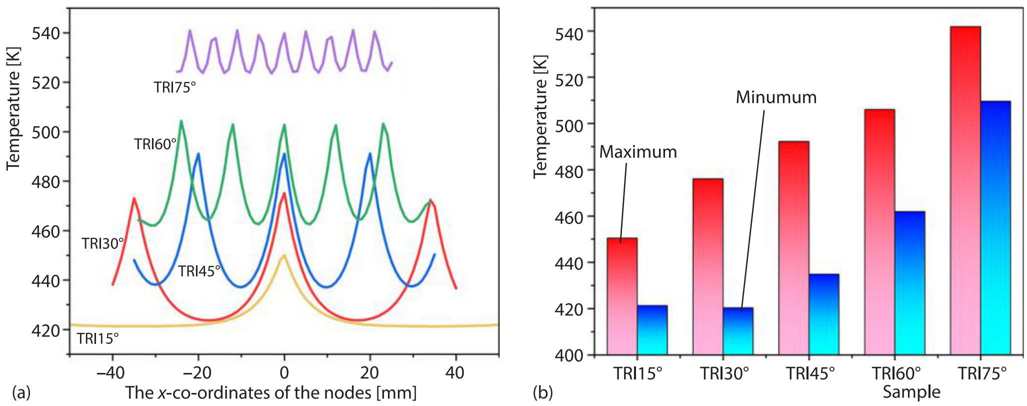

Figure 10. (a) Simulation temperature curves of the triangle-shape's composites with different degrees of the triangle's base angles and (b) maximum and minimum temperature of the top surface of the triangle-shape's composites with different degrees of the base angles

As can be seen from fig. 10(b), as the degree of the base angle increases, the values of maximum and minimum temperatures increase together. It is because with the increase of the base angle's degree, the length of the intermediate connecting layer will become shorter, which makes the path of heat transfer from the bottom surface to the top surface become shorter, causing more heat to reach the top surface. In addition, as the base angle's degree increases, the length of the baseline on the top surface decreases, so that the heat from the top surface sutures is more likely to reach the sutures on either sides and the middle of the baseline, so that the minimum temperature is in the middle of the baseline and the maximum temperature is on the suture increase.

The degree of the trapezoid's base angle

The simulation temperature curves of the selected nodes on the top surface of the trapezoid-shape's composites with different degrees of the base angles are shown in fig. 11(a). As can be seen from the figure, the maximum temperature occurred on the suture of the top surface of the composites, and the minimum temperature occurred in the middle of the trapezoid's baseline on the top surface.

It can be seen from fig. 11(b), with the increase of the base angle's degree, both the maximum and minimum temperatures of the top surface will increase. This is because as the base angle's degree increases, the heat transfer path from the bottom surface to the top surface becomes shorter, resulting in more heat reaching the suture on the top surface. The length of the trapezoid's topline on the upper surface of the composite are consistent, so the increase of the degree of the base angle will reduce the length of trapezoid's baseline on the upper surface, thus making it easier for the heat to reach the suture on the top surface and the middle of the baseline on the top surface, which causes the increasing the maximum and minimum temperatures of the top surface.

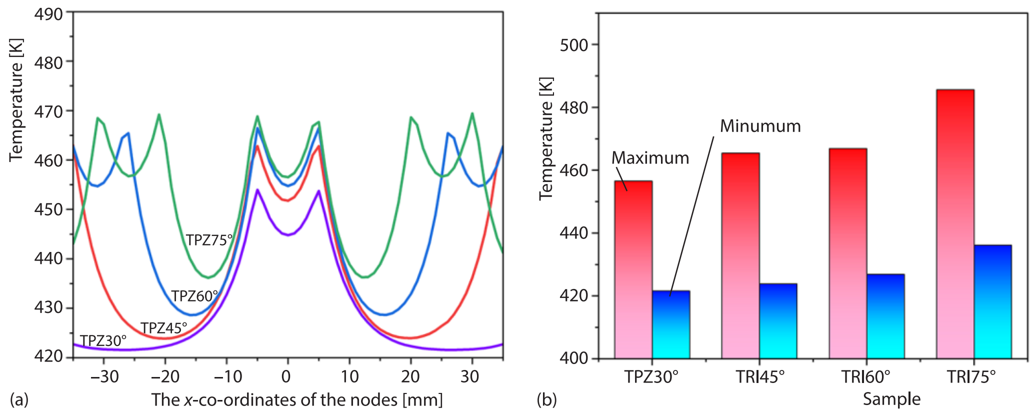

Figure 11. (a) Simulation temperature curves of the trapezoid-shape's composites with different degrees of the base angles and (b) maximum and minimum temperature of the top surface of the trapezoid-shape's composites with different degrees of the base angles

The length of the trapezoid's topline

The simulation temperature curves of the selected nodes on the top surface of the trapezoid-shape's composites with different lengths of trapezoid's toplines are shown in fig. 12(a), and the maximum and minimum temperature of the top surface of composites with different lengths of trapezoid's toplines are shown in fig. 12(b). When the lengths of trapezoid's topline of the top surface were greater than or equal to 10 mm, the maximum temperature of the top surface of the composite did not change very much. This is because when the base angle is constant, the length of the path of heat transfer from the bottom layer to the top layer is also constant, and the temperature on the sutures at either end of the toplines has little influence on each other, thus the maximum temperature on the suture is approximately steady. Since the minimum temperature occurs in the middle of the trapezoid's baseline of the top surface, and the fixed base angle makes the length of the trapezoid's baseline also more enough, the minimum temperature does not change much.

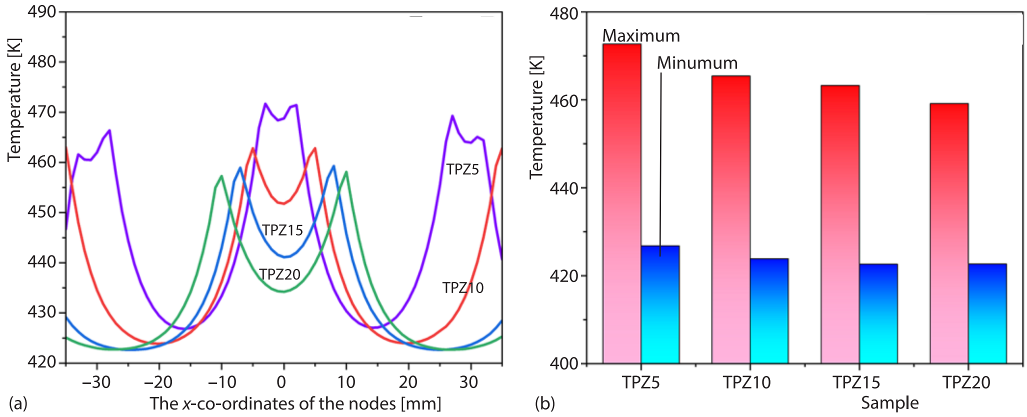

Figure 12. (a) Simulation temperature curves of the trapezoid-shape's composites with different lengths of the toplines and (b) maximum and minimum temperature of the top surface of the trapezoid-shape's composites with different lengths of the toplines

Conclusions

The thermal insulation performance of spacer fabric composites with different spacer shapes and different geometric parameters was studied in this paper. Through the comparative analysis of the heat transfer of spacer fabrics with different spacer shapes and geometric parameters by numerical simulation and experiment, the conclusions are as follows.

- The temperature distributions on the top surface of the spacer fabric composites with three spacer shapes were close to the numerical simulation results at high temperature, and the maximum relative error between the simulated value and the experimental value was about 4.8%, which indicates that the heat transfer simulation in this paper have certain predictive ability for the thermal insulation of spacer fabric composites.
- The heat transfer results of composite materials with triangular and trapezoidal spacers with different base angle's degrees were simulated and analyzed. It was found that the increase of the base angle will reduce the heat transfer path in the vertical direction, resulting in the increase of the maximum temperature of the top surface.
- The heat transfer results of composite materials with rectangular and trapezoidal spacers with different length side's lengths and topline's lengths were simulated and analyzed. It was found that the distance between two adjacent sutures on the top surface will affect the minimum temperature of the top surface, and as this distance goes up, the effect gets smaller and smaller. The maximum temperature would also be affected when the distance was small enough which makes the maximum temperature increase.

Acknowledgment

The work received financial support from National Natural Science Foundation of China (Grant No. 52107024), National Natural Science Foundation of China (Grant No. 52001245), and the Natural Science Foundation of Shaanxi Provincial Department of Education (No. 21JK0645).

References

[1] Xiaogang, C., *et al*., An Overview on Fabrication of 3-D Woven Textile Preforms for Composites, *Textile Research Journal*, *81* (2011), 9, pp. 932-944
[2] Yip, J., Ng, S.-P., Study of 3-D Spacer Fabrics, *Journal of Materials Processing Technology*, *206* (2008), 1-3, pp. 359-364
[3] Ai, S., *et al*., Effect of Stitch on Thermodynamic Properties of Sandwiched Thermal Protection Structures, *Composite Structures*, *99* (2013), May, pp. 41-47
[4] Asayesh, A., *et al*., Prototyping and Analyzing Physical Properties of Weft Knitted Spacer Fabrics as a Substitute for Wound Dressings, *The Journal of The Textile Institute*, *110* (2019), 9, pp. 1246-1256
[5] Umair, M., *et al*., Effect of Pile Height on the Mechanical Properties of 3-D Woven Spacer Composites, *Fibers and Polymers*, *20* (2019), 6, pp. 1258-1265
[6] Dehghan, N., *et al*., Introducing a Novel Model for Predicting Effective Thermal Conductivity of Spacer Fabrics Based on Their Structural Parameters, *Journal of Thermal Analysis and Calorimetry*, *147* (2021), 12, pp. 6615-6629
[7] Geerinck, R., *et al*., One-Shot Production of Large-Scale 3-D Woven Fabrics with Integrated Prismatic Shaped Cavities and Their Applications, *Materials and Design*, *165* (2019), 107578
[8] Sun, Y., *et al.*, Preparation and Characterization of 3-D Flexible High-Distance Spacer Fabric/Foam Composite, *Composite Structures*, *261* (2021), 113549
[9] Yang, Y., Hu, H., Spacer fabric-Based Exuding Wound Dressing – Part I: Structural Design, Fabrication and Property Evaluation of Spacer Fabrics, *Textile Research Journal*, *87* (2016), 12, pp. 1469-1480
[10] Ziaei, M., Ghane, M., Thermal Insulation Property of Spacer Fabrics Integrated by Ceramic Powder Impregnated Fabrics, *Journal of Industrial Textiles*, *43* (2012), 1, pp. 20-33
[11] Neje, G., Behera, B. K., Lateral Compressive Properties of Spacer Fabric Composites with Different Cell Shapes, *Applied Composite Materials*, *25* (2018), 4, pp. 725-734
[12] Neje, G., Behera, B. K., Influence of Cell Geometrical Parameters on the Mechanical Properties of 3d Integrally Woven Spacer Sandwich Composites, Composites – Part B: *Engineering*, *182* (2020), 107659
[13] Wang, H., Sun, R., Study on Thermal Insulation Properties of Spacer Fabric Reinforced Composites (in Chinese), *Synthetic Fiber in China*, *49* (2020), 12, pp. 44-48
[14] Sun, D., Preparation of TiO_2 Doped Silicon Aerogels and Study on the High Temperature Thermal Insulation, Ph. D. thesis, Properties Chang'an University (in Chinese), Xi'an, China, 2012
[15] Yue, C., Preparation and CO_2 Adsorption Performance of Amine-Loaded Silica Aerogel, Ph. D. thesis, National University of Defense Technology (in Chinese), Changsha, China, 2013
[16] Liu, T., *et al*., Numerical Simulation and Experiment Verified for Heat Transfer Processes of High-Property Inorganic Fiber Woven Fabrics, *Textile Research Journal*, *92* (2022), 13-14, pp. 2368-2378
[17] Zheng, Z., *et al*., Simulation of Heat Transfer through Woven Fabrics Based on the Fabric Geometry Model, *Thermal Science*, *22* (2018), 6B, pp. 2815-2825

Paper submitted: September 17, 2022
Paper revised: December 14, 2022
Paper accepted: December 20, 2022